The electrochemistry of selected lanthanides in the LiF-BeF_2 system

Martin Straka, Lórant Szatmáry
Department of Fluorine Chemistry, Nuclear Research Institute Řež plc, Czech Republic

Abstract

Among other applications, electrochemically based separation of actinides and lanthanides from molten salt media seems to be a suitable method for the reprocessing of spent nuclear fuel in proposed future types of nuclear reactors such as molten salt reactor. One of the most interesting features of the MSR concept is the circulation of the liquid molten fluoride fuel mixture. It allows the fuel to be continuously ("on-line") reprocessed, as is necessary for continuous reactor operation. The pyrochemical separation processes seem suitable for the "on-line" reprocessing technology and electrochemical separations are one of the most promising methods for the separation of fissile material and fission products. This work is focused on the electrochemical behaviour of several lanthanides (Sm, Gd) in FLiBe on inert (Mo, Mo) and reactive (Ni) electrodes. Electrochemical behaviour was studied by cyclic voltammetry and in the case of gadolinium, the electrolytic product was analysed by SEM-EDX analysis. Specific interactions between rare earth elements and polymer-like structure of Be-based melt were taken into account and experimental results interpreted. An evaluation of the possibilities of lanthanide recovery on the reactive electrode (Ni) is presented.

Introduction

Among other applications, electrochemically based separation of actinides and lanthanides from molten salt media seems to be a suitable method for the reprocessing of spent nuclear fuel in proposed future types of nuclear reactors such as molten salt reactor (MSR, proposed by Generation-IV International Forum as one of its six highlighted concepts [1]). One of the most interesting features of the MSR concept is the circulation of the liquid molten fluoride fuel mixture. It allows the fuel to be continuously ("on-line") reprocessed, as is necessary for continuous reactor operation. The non-water (pyrochemical) separation processes seem suitable for the "on-line" reprocessing technology and electrochemical methods, and, together with molten salt/liquid metal extraction [2], are among the most promising methods for the separation of fissile material and fission products. The history and present status of the MSR concept development are reviewed in [3]. To manage the reprocessing part of the MSR fuel cycle, it is necessary to have a knowledge of the thermodynamic data and electrochemical behaviour of the supposed fissile material and fission products in the molten salt media. This work is focused on the electrochemical behaviour of several lanthanides in the molten mixture of LiF and BeF_2 because the combination of neutronic, thermal and other physicochemical properties of these melts is making BeF_2-base salts a primary choice for MSR concepts.

Because of a narrow electrochemical window of LiF-BeF2 melt, other fluoride melts like LiF-CaF_2 are apparently more suitable over LiF-BeF_2 for electrochemical separations due to their higher electrochemical stability. Chamelot *et al.* [4] converted Gibbs energy data of pure solid compounds for NdF_3, SmF_2 and GdF_3 to standard potentials showing that those potentials lay in a more negative area than the decomposition of LiF-BeF_2 melt. However, as mentioned above, LiF-BeF_2 is considered a primary choice for MSR concepts. For this reason, a knowledge of the electrochemical behaviour of fission and fissile material in LiF-BeF_2 is important. Moreover, the difference between lanthanides electrochemistry in LiF-CaF_2 and LiF-BeF_2 should be studied because of the special nature of LiF-BeF_2 melt. While LiF is a typical ionic salt, BeF_2 forms a polymeric, high-viscosity liquid [5]. From the above it can be concluded that it is not possible to directly observe the deposition of lanthanides on inert electrodes. Only preceding reduction steps (where existing) can be observed in LiF-BeF_2 melt. Also, the deposition on the reactive electrode is an option as an alloy formation will have a depolarisation effect.

In this work, the electrochemistry of samarium on Mo electrode and the electrochemistry of gadolinium on the reactive Ni electrode was considered. An electrolytic experiment in the LiF-BeF_2-GdF_3 system was conducted and the resulting deposit was analysed by the SEM-EDX method.

Experimental

Chemicals

LiF (99.5%) was dried in a vacuum dryer at gradually increasing temperatures 100-150-250°C. BeF2 was analysed for an impurity by ICP-MS. Beryllium concentration was found to be 178.81 mg/g. The most important impurities were Si (0.699 mg/g) and Pb (0.107 mg/g). SmF3 (99.90%) was introduced into the melt in the glovebox under dry nitrogen atmosphere. 1 mm diameter Mo wire with a purity of 99.95% and Pt wire (0.5 mm diameter, better than 99.90 %) were used as working and comparison electrode, respectively.

Carrier melt

The phase diagram of LiF–BeF_2 melt has been studied by several authors in the past mainly by techniques of thermal analysis [6-12]. A phase diagram shows two eutectic points, the lowest melting point (T = 638.0 K) corresponds to x(BeF_2) = 0.52, the second eutectic is defined by x(BeF_2) = 0.34 with melting temperature T = 732.3 K [13]. Due to its low melting temperature, the area of LiF–BeF_2 compositions between two eutectic points is most interesting for applications of LiF-BeF_2 melt. Concentration and temperature dependences of several physicochemical properties have also been studied in the past. A summary of the available knowledge of LiF–BeF_2 density, viscosity, heat capacity, thermal conductivity and vapour pressure can be found in [13].

The concentration dependence of viscosity could be an important parameter for the practical use of the melt as there is a significant increase of viscosity with BeF_2 amount in the melt. At 813 K, the viscosity of LiF–BeF_2 with 31 molar % is 1.02 x 10-2 Pa.s. For the LiF–BeF_2 mixture with 50 molar % of BeF_2, viscosity increases to 3.75 x 10-2 Pa.s [14].

The density of liquid LiF–BeF_2 has been measured by Blanke *et al.* [15] and Cantor *et al.* [16] for several compositions. The molar volume values calculated from experimental densities show nearly ideal behaviour. The applicability of the additivity principle has also been confirmed for other molten salts [17] and an estimation method based on additivity principle has been presented by Khokhlov *et al.* [18]. The additivity of molar volumes is important when ternary mixtures are used, as is the case with this work. However, data for pure compounds are either limited or there are significant discrepancies in literature values. Extrapolation of experimental data to temperatures lower than the melting point of a pure compound will add another uncertainty to the calculation. In this work, the eutectic mixture of x(BeF_2) = 0.34 was used.

Experimental set-up

Electrochemical experiments were carried out in the cell (glassy-carbon crucible) placed in a nickel electrolyser consisting of a vessel closed by a removable flange with built-in holders for the electrodes, thermocouple and inlet and outlet of argon gas. The system is under argon atmosphere (99.998%) during the measurement. A resistance oven heats the electrolyser providing a homogenous thermal field up to 1 000°C. The whole apparatus is placed inside a glovebox with dry nitrogen atmosphere (99.95%); the dew point analyser monitors the level of moisture. The typical moisture content in the glovebox is under 5 ppm. A three-electrode system was used for all measurements. A large-surface glassy-carbon crucible was used as a counter electrode. Molybdenum wire (1 mm diameter) was used as working electrode. A quasi-reference Pt wire (0.5 mm) electrode was used. The electrodes were connected to HEKA PG 310 potentiostat (HEKA GmbH, Lambrecht, Germany) controlled by a PC with original software.

Results and discussion

An experimental study of the electrochemistry of samarium and gadolinium in LiF-BeF_2 melt was done on inert Mo (samarium) and Ni (gadolinium) electrode. Due to the narrow electrochemical window of LiF-BeF_2, only the first reduction step (one-electron exchange) was experimentally accessible in the case of samarium. In the case of the LiF-BeF_2-GdF_3 system, presumably some alloying effects took place. The electrolytic experiment conducted in the case of the LiF-BeF_2-GdF_3 system and the deposit was described by SEM analysis.

Samarium

Basic electrochemistry of samarium (Sm was introduced to the system in form of SmF_3) in LiF-BeF_2 was studied by cyclic voltammetry and chronopotentiometry in the

temperature range 804 K-872 K. Results were compared to those obtained in LiF-CaF_2 and chloride systems. Diffusion coefficients in the applied temperature range were calculated from the experimental data. A detailed view on elechtrochemical behaviour of samarium in LiF-BeF_2 melt can be found in [19]. Also, Massot *et al.* investigated the electrochemistry of Sm^{3+} ions in LiF-CaF_2 melt [20], which was described as a two-step mechanism with Sm^{2+} as an intermediate product. Gibilairo *et al.* [21] has studied co-deposition of samarium and Al on W electrode in the form of Sm-Al alloys.

Cyclic voltammetry was carried out on molybdenum electrode in LiF-BeF_2-SmF_3 melt at 804 K, 833 K, 847 K and 872 K. Molybdenum is an inert material with regard to samarium [22]. The cyclic voltammograms obtained at different scan rates on Mo electrode at 804 K are shown in Figure 1. The cyclic voltammogram exhibits one peak in the cathodic run at -0.48 V (vs. Pt reference) and its anodic counterpeak at -0.32 V (vs. Pt reference). Dependences of peak potential values on the logarithm of the potential sweep rate and peak current values on square root of the potential sweep rate were evaluated. As can be seen in Figures 2 and 3, peak potential values do not change significantly with the increase of the scan rate and it shows the linear dependence of the cathodic peak current, I_C, and the anodic peak current, I_A, on the square root of the sweep rate. This is the behaviour expected for a diffusion controlled process. The influence of temperature in the electrochemical behaviour of Sm^{3+} ions was studied in the temperature range 804 K -872 K. Potential peak values shift to more positive values with increasing temperatures. Also, a slight deviation of the current peak ratio I_C/I_A from unity was observed at 847 K and 872 K. It means that the reaction slightly deviates from reversibility at higher temperatures. A similar temperature dependence of the reversibility has been observed by Cordoba *et al.* [23] in the LiCl-KCl-SmF_3 system in the temperature range 723 K-873 K.

The number of exchanged electrons for the reaction was calculated by means of equation (1) [24]:

$$E_p^A - E_p^C = 2.22RT / zF \qquad (1)$$

where E_p^C is the potential of the cathodic peak, E_p^A is the potential of the anodic peak, R is the universal gas constant 8.314 $J.K^{-1}mol^{-1}$, T is the temperature, z is the number of exchanged electrons and F is the Faraday constant 96 500 $C.mol^{-1}$. The average value of z calculated from the results of five experiments at 804 K was 0.95. It can be concluded that one electron exchange occurs according to reaction $Sm^{3+}+e^- \rightarrow Sm^{2+}$.

Figure 1: Cyclic voltammograms of the LiF-BeF_2-SmF_3 system at different scan rates (50 mV/s to 250 mV/s with 50 mV/s step)

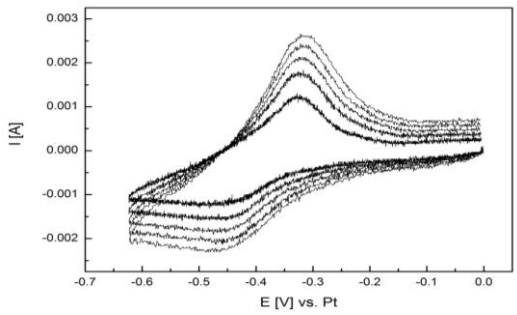

T=812 K. Working electrode: Mo wire (S=0.16 cm^2); Reference electrode: Pt wire; Auxiliary electrode: glassy-carbon crucible. [Sm^{3+}]=1.26 $mol.cm^{-3}$.

Figure 2: Variation of the cathodic and anodic peak potential as a function of the sweep rate in LiF-BeF$_2$ at 812 K

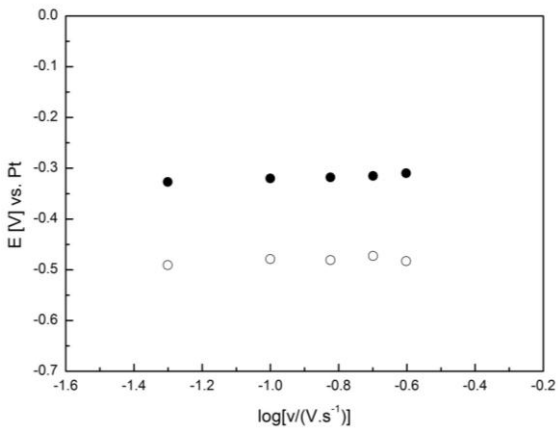

Working electrode: Mo wire (S=0.16 cm^2); Reference electrode: Pt wire; Auxiliary electrode: glassy-carbon crucible. [Sm^{3+}]=1.26 mol.cm^{-3}.

The cathodic peak current was correlated with the square root of potential scan rate by Randels-Sevcik Equation:

$$I_P = -0.4463 zFSC^0 \sqrt{\frac{zFD}{RT}} \sqrt{v} \qquad (3)$$

where I_p is cathodic peak current (A), S is the electrode surface (cm^2), c is the solute concentration (mol.cm^{-3}), D is diffusion coefficient (cm^2.s^{-1}) and v is potential scan rate (V.s^{-1}). The slope values of cathodic peak current – square root of potential scan rate dependence were determined:

$$\frac{I_p}{v} = -3.86 \times 10^{-3} As^{1/2} V^{-1/2} \text{ at 804 K} \qquad (4)$$

$$\frac{I_p}{v} = -5.14 \times 10^{-3} As^{1/2} V^{-1/2} \text{ at 833 K} \qquad (5)$$

$$\frac{I_p}{v} = -6.35 \times 10^{-3} As^{1/2} V^{-1/2} \text{ at 847 K} \qquad (6)$$

$$\frac{I_p}{v} = -7.02 \times 10^{-3} As^{1/2} V^{-1/2} \text{ at 872 K} \qquad (7)$$

Slope values are valid for S=0.16 cm^2 and C^0=1.26x10^{-4} mol.cm^{-3}.

Figure 3: Variation of cathodic and anodic peak current as a function of the potential scan rate

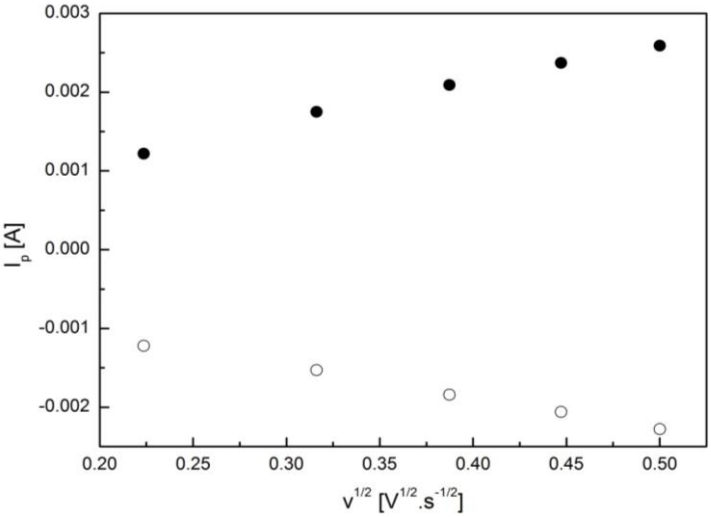

Working electrode: Mo wire (S=0.16 cm^2); Reference electrode: Pt wire; Auxiliary electrode: glassy-carbon crucible. [Sm^{3+}]=1.26 mol.cm^{-3}.

Diffusion coefficients of Sm^{3+} ions in LiF-BeF$_2$ melt in the temperature range 804 K-872 K were determined using cyclic voltammetry from Randels-Sevcik Equation. Table 1 reports values of diffusion coefficient in the temperature range 804 K-872 K.

Results obey Arrhenius´ law (Equation 13):

$$D = D^0 \exp\left(\frac{-E_a}{RT}\right) \qquad (13)$$

where E_a is the activation energy. Evolution of *ln*D versus 1/*T* was found to be linear (see Figure 7):

$$\ln D = 1.9549 - \frac{12.3258}{T} \qquad (14)$$

From Equation 14, the value of activation energy was calculated to be 102.5 kJ/mol.

Table 1: Diffusion coefficients of SmF$_3$ in LiF-BeF$_2$ melt calculated from cyclic voltammetry (CV)

T [K]	*Method*	*D [cm^{2}s^{-1}]*
804.1	CV	1.37x10^{-6}
832.7	CV	2.52x10^{-6}
846.5	CV	3.94x10^{-6}
872.2	CV	4.91x10^{-6}

Diffusion coefficients of Sm^{3+} ions in LiF-BeF_2 melt are of the magnitude of 10^{-6} cm^2s^{-1} (see Table 1). Sm^{3+} diffusion coefficient values in BeF_2-free melt (LiF-CaF_2) have been measured by Massot *et al.* [20] in the temperature range 1 100 K-1 170 K. Although the temperature range is different from that in this work, extrapolated values are surprisingly similar with respect to the different nature of BeF_2 compared to other components (see Figure 4). High diffusion coefficients of several actinides in lanthanides obtained in LiF-BeF_2 despite its special structure and high viscosity have also been reported by Moriyama *et al.* [25]. For uranium, diffusion coefficients have been reported by Manning and Mamantov [26] and Straka *et al.* [27] with similar conclusions. A possible explanation was given by Moriyama *et al.* [25]; a considerable fraction of polymeric species $Be_mF_n^{2m-n}$ is present, with the result that the system is not homogeneous and some paths of the diffusing species are preferred.

Figure 4: Linear relationships of the diffusion coefficients of Sm^{3+} ions with temperature in LiF-BeF_2 melt ● – this work) and LiF-CaF_2 (○ - Massot *et al.* [20])

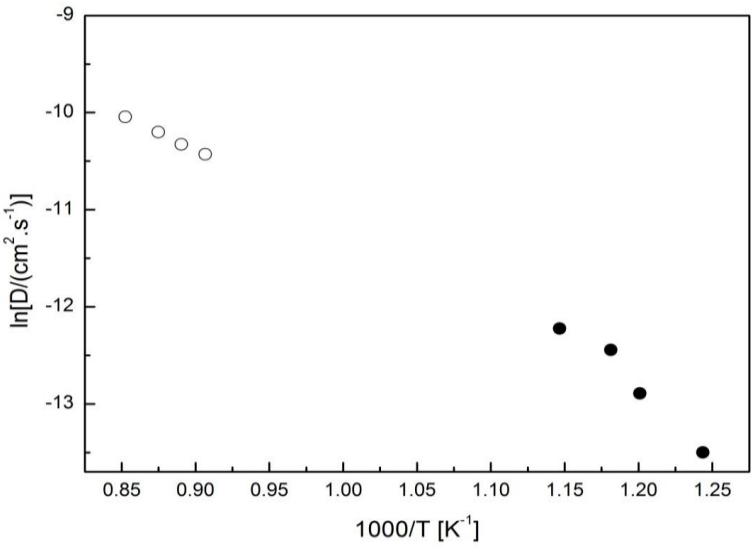

Gadolinium

The electrochemistry of gadolinium was studied on Ni electrode. The electrochemistry of gadolinium has been studied by Nourry *et al.* [28]. Electroreduction of Gd^{3+} ions in LiF-CaF_2 system on inert Ta electrode was described as a one-step process with three electrons exchanged. Also, Nourry has published two papers dealing with gadolinium deposition on Ni and Cu reactive electrodes [29] [30], confirming the alloying reactions. Figure 5 shows cyclic voltammogram of the LiF-BeF_2-GdF_3 system on Ni electrode. As can be seen, several effects can be observed on both the cathodic and the anodic sides.

Figure 5: Cyclic voltammogram of the LiF-BeF_2-GdF_3 system at 50 mV/s

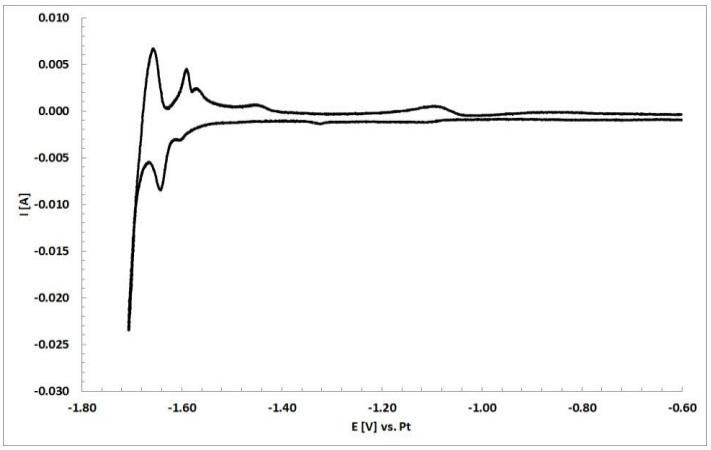

T=823 K. Working electrode: Mo wire (S=0.16 cm^2); Reference electrode: Pt wire; Auxiliary electrode: glassy-carbon crucible. [Gd^{3+}]=1.26 mol.cm^{-3}.

It was assumed that Gd is the subject of alloying reactions with Ni. Also, it is known that lanthanides are able to form at least a $LnBe_{13}$ type of compounds [31]. Open-circuit chronopotentiometric measurement was done in order to further verify the formation of intermetallic compounds. The measurement is shown in Figure 6. Several plateaus typical of equilibrium between two intermetallics in the solid state can be observed.

Potentiostatic electrolysis at -1.65 V vs. Pt (see Figure 5 for comparison) was applied for 7 200 s at 823 K on Ni wire electrode. The cross-section of the electrode was later analysed by SEM analysis. (see Figure 7). In the picture, Ni electrode can be seen, a thin dark layer and a thick white layer on it. EDX analysis revealed the presence of Ni, Gd in the dark layer and the presence of Gd in the white layer. It is in agreement with the mechanism of Gd-Ni alloy formation, on which gadolinium is then deposited. However, one should have in mind the limitations of the used EDX method. As beryllium is a very light element, its reliable detection is not possible. Because of that, the possibility of the re-definition of the products to Gd-Be-Ni and Gd-Be alloys cannot be excluded. Further investigation of the product structure is desirable.

Figure 6: Open-circuit chronopotentiogram of the LiF-BeF2-GdF3 system on Mo electrode at T=923 K

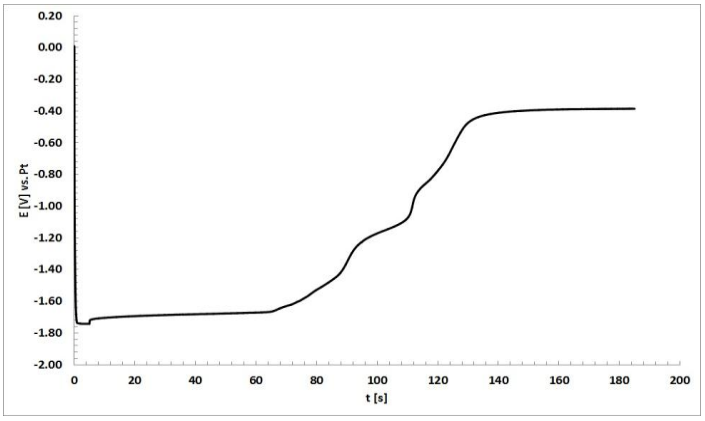

Auxiliary electrode: glassy carbon; reference electrode: Pt wire.

Figure 7: SEM picture of Ni electrode cross-section after the electrolytic deposition of Gd

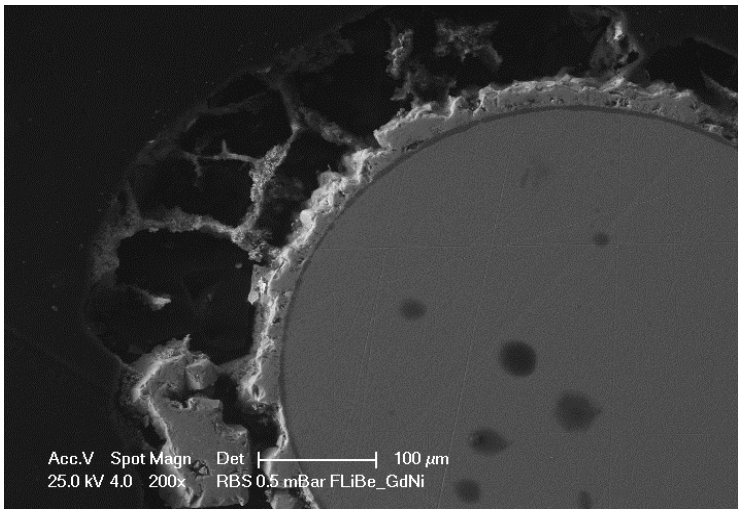

Conclusion

The electrochemistry of samarium and gadolinium in LiF-BeF$_2$ melt was investigated by cyclic voltammetry. The electrochemical reduction of Sm^{3+} ions to Sm^{2+} ions was studied on inert Mo electrode. The process was described as diffusion-controlled. The temperature dependence of the Sm^{3+} diffusion coefficient was measured in the temperature range 804 K-872 K. The dependence obeys Arrhenius law. Activation energy was calculated to be 1 02.5 kJ/mol. The diffusion coefficients can be extrapolated to temperatures in which their values are known for Sm^{3+} ions in Be-free fluoride melts. The extrapolated values seem to be similar against the expectations as Be-based melts are different in their nature. The explanation can be based on the assumption that the melt is not strictly homogenous and different paths for an electroactive species are possible.

Cyclic voltammograms of the LiF-BeF2-GdF3 system on Ni electrode were measured. Effects on cathodic and anodic sides suggest that alloys were formed. This was supported also by an open-circuit chronopotentiometry measurement. The deposit obtained during 7 200 s electrolysis was analysed by SEM-EDX analysis. The deposited products were easily recognisable, however, further investigation will be necessary in order to confirm the structure of these products, i.e. whether Be is a component of these products.

Acknowledgements

This work was supported by the Ministry of Industry and Trade of the Czech Republic.

References

[1] A Technology Roadmap for Generation IV Nuclear Energy Systems, US-DOE Nuclear Energy Research Advisory Committee and the Generation-IV International Forum, December 2002; GIF-002-00, http://gif.inel.gov.

[2] M.W. Rosenthal (1974), Recent progress in molten salt reactor development. Technical report ORNL-5018 Oak Ridge National Laboratory.

[3] J. Uhlir (2007), Chemistry and technology of Molten Salt Reactors – history and perspectives. *J Nucl Mat*; 360:6-11.

[4] P. Chamelot, L. Massot, C. Hamel, C. Nourry, P. Taxil (2007), Feasibility of the electrochemical way in molten fluorides for separating thorium and lanthanides and extracting lanthanides from the solvent. *J Nucl Mat;* 360:64-74.

[5] AL. Mathews, CF. Baes (1968), Oxide Chemistry and Thermodynamics of Molten LiF-BeF2 Solutions. *Inorg Chem;* 7:373.

[6] E. Thilo, H-A. Lehmann (1949), Chemische Untersuchungen von Silikaten. XII. Über das System LiF-BeF2 und seine Beziehungen zum System MgO-SiO2. *Zeit Anorg Chem*; 258:332-355.

[7] DM. Roy, R. Roy, EF. Osborn (1950), Phase Relations and Structural Phenomena in the Fluoride-Model Systems LiF-BeF2 and NaF-BeF2. *J Am Ceram Soc;* 33:85-90.

[8] DM. Roy, J. Roy, EF. Osborn (1954), Fluoride Model Systems IV. The Systems LiF-BeF2 and RbF2-BeF2. *J Am Ceram Soc*; 37:300.

[9] AV. Novoselova, EI. Simanov, EI. Jarembash (1952), Thermal and X-ray Analysis of the Lithium- Beryllium Fluoride System. *Zh Fiz Khim;* 26:1244.

[10] LV. Jones, DE. Etter, CR. Hudgens *et al.* (1962), Phase Equilibria in the Ternary Fused-Salt System LiF-BeF2-UF4. *J Am Ceram Soc;* 45:79-83.

[11] RE. Thoma, H. Insley, HA. Friedman, GM. Hebert (1968), Equlibrium Phase Diagram of Lithium Fluoride-Beryllium Fluoride-Zirconium Fluoride System. *J Nucl Mat;* 27:166.

[12] R.E. Thoma, J. Braunstein (1972), New Electrochemical Measurements of Liquidus in LiF-BeF2 System - Congruency of Li2BeF4. *J Phys Chem;* 76:1154.

[13] O. Benes, RJM. Konings (2009), Thermodynamic properties and phase diagrams of fluoride salts for nuclear applications. *J Fluor Chem*; 130:22-29.

[14] JA. Lane, HG. MacPherson, F. Maslan (1958), Fluid Fuel Reactors: Addison-Wesley.

[15] BC. Blanke, EN. Bousquet, ML. Curtis, EL. Murphy (1956), Density and Viscosity of Fused Mixtures of Lithium, Beryllium and Uranium Fluorides. *Technical Report* MLM-1086, Mound Laboratory.

[16] S. Cantor, WT. War, CT. Moynihan (1969), Viscosity and Density in Molten BeF2–LiF Solutions. *J Chem Phys;* 50:2874-2879.

[17] JPM. Van der Meer, RJM. Konings (2007), Thermal and physical properties of molten fluorides for nuclear applications. *J Nucl Mat;* 360:16-24.

[18] V. Khokhlov, V. Ignatiev, V. Afonichkin (2009), Evaluating physical properties of molten salt reactor fluoride mixtures. *J Fluor Chem* 2009; 130:30-37.

[19] M. Straka, M. Korenko, F. Lisý, L. Szatmáry (2011), Electrochemistry of samarium in lithium-beryllium fluoride salt mixture. *J Rare Earths;* 29:798-803.

[20] L. Massot, P. Chamelot, P. Taxil (2005), Cathodic behaviour of samarium(III) in LiF-CaF2 media on molybdenum and nickel electrodes. *Electrochim Acta*; 50:5510-5517.

[21] M. Gibilaro, L. Massot, R. Chamelot, P. Taxil (2009), Co-reduction of aluminium and lanthanide ions in molten fluorides: Application to cerium and samarium extraction from nuclear wastes. *Electrochim Acta*; 54:5300-5306.

[22] B. Predel, Mo-Sm (Molybdenum-Samarium). The Landolt-Bronstein Database, doi:10.1007/10522884_2098.

[23] G. Cordoba, C. Caravaca (2004), An electrochemical study of samarium ions in the molten eutectic LiCl plus KCl. *J Electroanal Chem*; 572:145-151.

[24] AJ. Bard, LR. Faulkner (1980), Electrochemical Methods, *Fundamentals and Applications*. New York, Wiley.

[25] H. Moriyama, K. Moritani, Y. Ito (1994), Diffusion-Coefficients of Actinide and Lanthanide Ions in Molten Li2BeF4. *J Chem Eng Data;* 39:147-149.

[26] D.L. Manning, G. Mamantov (1974), Studies on Electroreduction of Uranium(IV) in Molten LiF-BeF2-ZrF4 by Square-Wave Voltammetry. *Electrochim Acta*; 19:177-179.

[27] M. Straka, M. Korenko, F. Lisy (2010), Electrochemistry of uranium in LiF-BeF2 melt, *J Radioanal Nucl Chem*; 284:245-252.

[28] C. Nourry, L. Massot, P. Chamelot, P. Taxil (2008), Data acquisition in thermodynamic and electrochemical reduction in a Gd(III)/Gd system in LiF-CaF2 media. *Electrochim Acta;* 53:2650-2655.

[29] C. Nourry, L. Massot, P. Chamelot, P. Taxil (2009), Electrochemical reduction of Gd(III) and Nd(III) on reactive cathode material in molten fluoride media. *J Appl Electrochem;* 39:927-933.

[30] C. Nourry, L. Massot, P. Chamelot, P. Taxil (2009), Neodymium and gadolinium extraction from molten fluorides by reduction on a reactive electrode. *J Appl Electrochem*; 39:2359-2367.

[31] U. Benedict, K. Buijs, C. Dufour, JC. Toussaint, Preparation and X-Ray Diffraction Study of PaBe13, AmBe13 and CmBe13. J Less-Comm Met 1975; 42:345-354.